Improved Instantaneous Frequency Estimation of Multi-Component FM Signals

Vaishali S. Amin [†], Yimin D. Zhang [†], and Braham Himed [‡]

[†] Department of Electrical and Computer Engineering, Temple University, Philadelphia, PA, 19122, USA
[‡] RF Technology Branch, Air Force Research Laboratory, AFRL/RYMD, Dayton, OH, 45433, USA

***Abstract*—In this paper, we address the problem of instantaneous frequency (IF) estimation of non-linear, multi-component frequency modulated (FM) signals in the presence of burst missing data samples, where different signal components have distinct amplitude levels. Burst missing data induce significant artifacts in the time-frequency (TF) representations of such signals, thus making identification of true IFs challenging. We propose a technique that involves local peak detection and filtering within a window at each time instant. The threshold for each local TF segment is adapted based on the local maximum values of the signal within the segment. The proposed approach not only mitigates the undesired impacts of the artifacts and cross-terms due to burst missing data samples, but also successfully resolves signal components with distinct amplitude levels and preserves a high resolution of the auto-terms. The effectiveness of the proposed method and its superiority over existing techniques are verified through simulation results.**

***Index Terms*—Adaptive local filtering, burst missing samples, directional time-frequency representation, non-stationary signal.**

I. Introduction

Many practical signals used in radar, sonar, biomedical applications, and wireless communications can be modeled as non-stationary frequency modulated (FM) signals [1], [2]. The time-frequency (TF) representation is widely accepted as the most preferred method to analyze, characterize, and process such signals [3], [4]. In practice, these signals often experience missing data samples due to various reasons, such as multipath fading, line-of-sight obstruction, and noise removal. The scenario of burst missing samples emerges when missing data occurs consecutively as a result of interference, obstruction, or fading that last for multiple sampling intervals. Burst missing data samples introduce artifacts that exhibit superimposed sinc-like patterns created around the true instantaneous frequencies (IFs) in the TF representations (TFRs) of such FM signals, and thus, present a more challenging situation for signal characterization and analysis [5] compared to the random missing sample case, in which artifacts are uniformly distributed in the TF domain [6].

Various compressive sensing and TF kernel based approaches have been proposed that address TFR reconstruction in the presence of random missing samples [6]–[10]. Data-dependent TF kernels, such as the adaptive optimal kernel (AOK) [11], and sparse reconstruction methods, such as the orthogonal matching pursuit (OMP) [12], are found to be effective in the case of random missing data samples. However, these methods alone fail to reliably reconstruct TFRs when missing data occurs in bursts. The problem of TFR reconstruction of mono-component non-linear FM signals in the presence of burst missing samples is considered in [13]. In this approach, the data interpolation/extrapolation-based missing data iterative adaptive approach (MIAA) [14] is used in the time-lag domain, which is stationary with respect to the lag index. While the MIAA performs well to iteratively reconstruct the TFR from the instantaneous autocorrelation function (IAF) using their one-dimensional (1-D) Fourier transform relationship, this approach exhibits excessive cross-terms in the case of multi-component FM signals in the presence of burst missing samples. A recently developed missing data iterative sparse reconstruction (MI-SR) approach [5], when applied in conjunction with signal-adaptive TF kernels, provides effective suppression of cross-terms and artifacts due to burst missing data samples, and thus, achieving reliable TFR recovery.

In the case of multi-component FM signals with high variation in their relative amplitude levels and in the presence of burst missing data samples, the aforementioned methods either fail completely to recover the weak signal components or demonstrate excessive artifacts and spurious signal signatures, thus misguiding identification of the true IFs. In this scenario, a recently developed adaptive directional TF distribution (ADTFD) [15] generally outperforms the existing approaches in terms of resolving close signal components with high variation in their relative amplitudes, while achieving a high resolution of auto-term TFRs. However, ADTFD too, suffers from problems of aliasing signal components, artifacts, and interfering cross-terms.

Pre-processing techniques may be employed for resolution enhancement, cross-term suppression, and de-noising of the TFRs to improve the reliability and performance of the underlying advanced methodologies in various applications such as detection, tracking, classification, and diagnosis [16]. One of the common techniques is to find peaks using well-known zero-derivative method and then smoothing the entire curve using a low-pass filter. However, doing so adversely affects the TFR resolution. In addition, accidental zero-crossings of the first derivative occur in noisy signals, leading to false peak detections.

To overcome such issues, in this paper, we propose a new

The work of V. S. Amin and Y. D. Zhang is supported in part by a subcontract with Matrix Research, Inc. for research sponsored by the Air Force Research Laboratory under contract FA8650-14-D-1722.

technique that involves local filtering of the TFR of a multi-component FM signal. At each time instant, peaks are first detected locally along the frequency axis within the window of a desired length. Then, the peaks having amplitudes higher than the threshold, specified as a percentage of the local maximum value, are retained, and low amplitude artifacts are filtered out. We observe that, at each time instant, the peaks associated with the true IFs usually assume maximum amplitudes, whereas the peaks due to undesired artifacts have much smaller amplitudes, within a window of an appropriate length. With this large difference in amplitudes of the true IFs and the artifacts in a local TF segment, by adapting the threshold based on local maximum values of the signal within that window, the local characteristics of the signal are well preserved and better represented. This is particularly useful when the signal consists of multiple close components in the TF domain but with significant differences in their amplitude levels. The proposed approach, referred to as adaptive local filtering-based directional time-frequency distribution (ALF-DTFD), offers multifold advantages, namely, effectively removing cross-terms and artifacts due to burst missing samples, hence preserving a high resolution of the true IFs, maintaining the maximum of the distribution properties, and enhancing feature extractions of the underlying TFRs. The proposed technique can be successfully applied to the multi-component FM signals having either uniform or random positions of missing data bursts that may contain the same or different numbers of missing data.

Notations. A lower (upper) case bold letter denotes a vector (matrix). $(\cdot)^{\mathrm{T}}$ and $(\cdot)^{*}$, respectively, represent transpose and complex conjugation. $\mathcal{F}_x(\cdot)$ and $\mathcal{F}_x^{-1}(\cdot)$, respectively, define the discrete Fourier transform (DFT) and inverse DFT (IDFT) with respect to x. $\lceil a \rceil$ denotes the ceiling function which returns the least integer greater than or equal to a.

II. Signal Model and Quadratic Time-Frequency Representations

A. Signal Model

Consider a discrete-time multi-component analytic FM signal, expressed as

$$s[t] = \sum_{k=1}^{K} a_k[t] \exp(j\phi_k[t]), \qquad t = 1, ..., T, \tag{1}$$

where K is the total number of components, $a_k(t)$ and $\phi_k(t)$ are, respectively, the slowly time-varying coefficient and time-varying phase of the kth component of the signal. The observed data contains a total number of N burst missing data samples with $N = \sum_{b=1}^{B} N_b,\ 0 \leq N < T$, where B is the total number of missing bursts, and N_b is the number of missing samples in the bth burst, $b = 1, ..., B$. The positions of the missing data bursts are assumed to be randomly distributed over time and different bursts are assumed to be mutually non-overlapping.

Let $\mathbb{S} \subset \{1, ..., T\}$ be the set of observed time instants with a cardinality of $|\mathbb{S}| = T - N$. As such, the observed signal, $r[t]$, can be expressed as the product of $s[t]$ and an observation mask, $R[t]$, i.e.,

$$r[t] = s[t] \cdot R[t], \tag{2}$$

where

$$R[t] = \begin{cases} 1, & \text{if } t \in \mathbb{S}, \\ 0, & \text{if } t \notin \mathbb{S}. \end{cases} \tag{3}$$

It should be noted that a random missing sample scenario could be considered as a special case of the underlying burst missing sample scenario with B equal to N and N_b equal to 1 in the above expressions.

B. Quadratic Time-Frequency Representations

The IAF of $r[t]$ is defined in the time-lag (t-τ) domain as

$$C_{rr}[t, \tau] = r\left[t + \tau\right] r^{*}\left[t - \tau\right]. \tag{4}$$

The ambiguity function (AF) is obtained by applying a 1-D DFT to the IAF with respect to time t, expressed as

$$A_{rr}[\theta, \tau] = \mathcal{F}_t[C_{rr}[t, \tau]] = \sum_{t} C_{rr}[t, \tau] e^{-\jmath 2\pi\theta t}, \tag{5}$$

where θ is the frequency shift.

On the other hand, the Wigner-Ville distribution (WVD) can be obtained by taking the 1-D DFT of the IAF with respect to τ as

$$W_{rr}[t, f] = \mathcal{F}_\tau[C_{rr}[t, \tau]] = \sum_{\tau} C_{rr}[t, \tau] e^{-\jmath 4\pi f \tau}. \tag{6}$$

Note that, in the above expression 4π is used instead of 2π, because integer valued τ is considered in (4).

III. Proposed Adaptive Local Filtering Based Approach

The WVD provides optimal representation of mono-component linear FM signals [3]. However, it generates excessive cross-terms in the case of multi-component signals or non-linear FM signals. It also suffers from non-local nature and possibility of non-positive energy distribution. These drawbacks of WVD motivated the development of reduced-interference distributions [16], [17] that attempt to mitigate the effects of the interfering cross-terms, while preserving the energy of the auto-terms with a high resolution.

A. Adaptive Directional Time-Frequency Distribution (ADTFD)

The ADTFD [15] is obtained by applying a locally adaptive 2-D smoothing kernel to the respective TF point of the underlying quadratic TFR. For the TFRs represented by $\chi[t, f]$, the corresponding ADTFD is given as

$$\chi_{\mathrm{adapt}}[t, f] = \chi[t, f] \underset{t}{*} \underset{f}{*} \psi_\theta[t, f], \tag{7}$$

where $\underset{t\,f}{**}$ denotes 2-D convolution with respect to both time index t and frequency index f, and $\psi_\theta[t, f]$ is the double derivative directional Gaussian filter (DD-DGF) defined as

$$\psi_\theta[t, f] = \frac{pq}{2\pi} e^{-p^2 t_\theta^2 - q^2 f_\theta^2} (1 - p^2 f_\theta^2), \tag{8}$$

where $t_\theta = t\cos(\theta) + f\sin(\theta)$, $f_\theta = f\cos(\theta) - t\sin(\theta)$, θ is the rotation angle with respect to the time axis, and p and q are parameters that control the spread of the DD-DGF respectively along the time and frequency axes. In order to suppress cross-terms while preserving the resolution of auto-terms, the direction of a smoothing kernel should remain aligned with the major axis of auto-terms and cross-terms. The direction of the DD-DGF is optimized locally for each TF point by maximizing the correlation of the directional kernel with the modulus of a underlying quadratic TFR, i.e.,

$$\theta[t,f] = \frac{2\pi}{L} \arg\max_{l} \left| |\chi[t,f]| \underset{t}{*}\underset{f}{*} \psi_{\theta_l}[t,f] \right|, \tag{9}$$

where $\psi_{\theta_l}[t,f]$ is the directional Gaussian kernel rotated by $\theta_l = 2\pi l/L$ radians along the time-axis in total L discrete steps, $l = 0, ..., L-1$. Note in the above expression that the modulus of the $\chi[t,f]$ is considered to avoid the oscillatory effects of the cross-terms.

While the WVD can be used in place of $\chi[t,f]$ in (7), in this paper, we use the smoothed pseudo WVD (SPWVD) [18], [19] for improved cross-term reduction. The SPWVD of the signal $s[t]$ is given by

$$\chi[t,f] = \sum_{u} g[u] \sum_{\tau} h[\tau]\; s[t-u+\tau]\, s^{*}[t-u-\tau]\, e^{-j4\pi f\tau}, \tag{10}$$

where $g[u]$ and $h[\tau]$ are, respectively, time and lag smoothing windows. The separable kernel in SPWVD facilitates independent optimization for the time and frequency smoothing, thus providing improved cross-terms suppression results.

B. Proposed Adaptive Local Filtering-based Directional Time-Frequency Distribution (ALF-DTFD)

Multi-component non-linear FM signals exhibit severe cross-terms between components. Additionally, burst missing samples introduce significant artifacts in the TFR of these signals, thereby increasing the possibility of erroneous detection, processing, and classification. In this section, we delineate the proposed adaptive local filtering-based approach, referred to as ALF-DTFD, that aims to mitigate the undesired effects of cross-terms and artifacts from the underlying TFRs.

We begin with the ADTFD, computed using (7)–(10), of the given multi-component FM signal. Both auto-terms and cross-terms appear as ridges in the TF domain. Using the operation defined in (9), the smoothing kernel of the ADTFD provides maximum output when it is parallel to these ridges, providing low-pass filter characteristics along its major direction. The output of the smoothing kernel is minimized in other directions, thus reducing the energy at TF points where no signal components are present. We observe that, after this operation, for each time instant, the maximum valued peaks generally belong to the true signal signatures, whereas the undesired artifacts assume low values within a local TF segment enclosed in a window of an appropriate length. The proposed ALF-DTFD technique, motivated by the above observation, offers low computational complexity and is found effective in suppressing cross-terms and artifacts due to burst missing data samples, while preserving the energy of the signal components with different amplitude levels.

Denote the column of the underlying TFR at time instant t as a $P \times 1$ vector $\mathbf{x}^{(t)} = [\chi_{\text{adapt}}[t,1], ..., \chi_{\text{adapt}}[t,P]]^{\text{T}}$, $t = 1, \ ..., \ T$, with P representing the total number of frequency-grid points. As all the steps are performed for each time instant, we omit superscript (t) in the sequel for notational simplicity.

Divide the vector $\mathbf{x}$ into M non-overlapping segments, with $Q = \lceil P/M \rceil$ being the number of elements in each segment, i.e.,

$$\mathbf{x} = \left[\mathbf{x}_1^{\text{T}}, \mathbf{x}_2^{\text{T}}, ..., \mathbf{x}_M^{\text{T}}\right]^{\text{T}}, \tag{11}$$

where the mth segment, $\mathbf{x}_m$, is given by

$$\mathbf{x}_m = \Big[x[(m-1)Q+1], ..., x[mQ]\Big]^{\text{T}}, \quad 1 \le m \le M. \tag{12}$$

If $MQ > P$, $MQ - P$ zeros are appended at the end of $\mathbf{x}$, i.e., in the last segment $\mathbf{x}_M$. The selection of M depends on the total number of components and their separation in the frequency domain. For a signal with few closely spaced components, a small value of M should be used (e.g., 1 or 2). For signals with a higher number of components, or when they spread in the entire frequency region, a higher value of M may be desired, without exceeding the total number of signal components.

The peaks are detected locally within each segment $\mathbf{x}_m$. A TF point is considered a peak if it has the maximum value, and is preceded by a value lower by the specified threshold, defined as a percentage of the maximum value. Denote $x_m[n]$ as the nth element of $\mathbf{x}_m$, and $\mathbb{P}_m$ as the set of the detected peaks within the segment $\mathbf{x}_m$. Then,

$$x_m[n] \in \mathbb{P}_m, \text{ if } |x_m[n]| - |x_m[n-1]| \ge \xi \max|\mathbf{x}_m|, \tag{13}$$

where $0 < \xi \le 1$, and $n = 2, ..., Q$. The value of ξ should be properly chosen. A small value of ξ will yield ineffective suppression of the undesired artifacts and cross-terms from the TF region, whereas a large value will aggressively remove auto-terms along with cross-terms.

The retained TF points represent the detected high-energy peaks, whereas low energy artifacts are filtered out. This is achieved by the following thresholding,

$$x_m[n] = \begin{cases} x_m[n], & \text{if } \ x_m[n] \in \mathbb{P}_m, \\ 0, & \text{otherwise.} \end{cases} \tag{14}$$

The entire procedure of proposed ALF-DTFD technique is summarized in Algorithm 1.

IV. Simulation Results

To demonstrate the effectiveness of the proposed ALF-DTFD approach, we consider a two-component FM signal with different amplitudes of the components, given by

$$y(t) = \exp(j\phi_1(t)) + 0.6\exp(j\phi_2(t)), \quad t = 1, ..., T, \tag{15}$$

where T is chosen to be 256 and the instantaneous phase laws of these two components are respectively expressed as,

$$\phi_1(t) = 0.05t + 0.000001t^3, \;\; \phi_2(t) = 0.25t - 0.0000005t^3. \tag{16}$$

Figs. 1(a)–1(e) respectively show the real part of the original signal without missing samples, and the corresponding IAF,

Algorithm 1: ALF-DTFD algorithm

Compute ADTFD of the received signal, $\chi_{\text{adapt}}[t,f]$, using (7)–(10);
Initialize the total number of frequency grid points P, total number of samples T, number of segments M, and threshold parameter ξ with $0 < \xi \leq 1$;
for $t = 1 : T$ **do**
  Divide $\mathbf{x} = \chi^{\text{T}}_{\text{adapt}}[t,:]$ into M non-overlapping segments, $\mathbf{x}_1, \mathbf{x}_2, ..., \mathbf{x}_M$, each of length $Q = \lceil P/M \rceil$;
  for $m = 1 : M$ **do**
    Initialize the set of the detected peaks within $\mathbf{x}_m$, $\mathbb{P}_m = \emptyset$;
    for $n = 2, ..., Q$ **do**
      if $|x_m[n]| - |x_m[n-1]| \geq \xi \max|\mathbf{x}_m|$ **then**
        $x_m[n] \in \mathbb{P}_m$;
      end if
    end for
    foreach $x_m[n] \in \mathbf{x}_m$ **do**
      if $x_m[n] \notin \mathbb{P}_m$ **then**
        $|x_m[n]| = 0$;
      end if
    end foreach
  end for
  $\chi_{\text{adapt}}[t,:] = \mathbf{x}[1:P]$;
end for

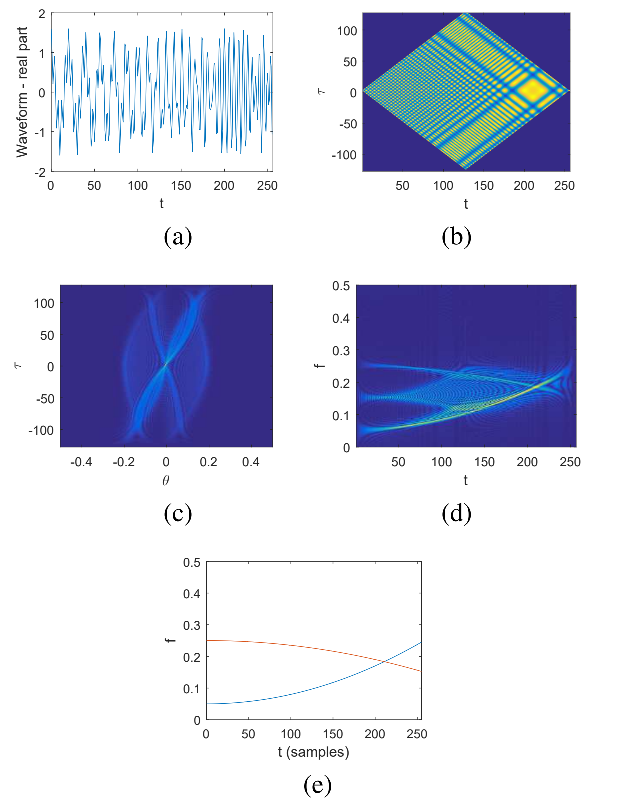

Fig. 1 The original signal without missing samples: (a) Real part of the signal; (b) IAF; (c) AF; (d) WVD; (e) True IFs.

AF, WVD, and true IFs. In Fig. 1(b), the IAF entries, related to the time at which the two signal components intersect in the TF region, assume maximum amplitudes. In Fig. 1(c), the two auto-term signatures pass through the origin and the cross-terms oscillates around the origin. The WVD depicted in Fig. 1(d) shows the excessive cross-terms even without any missing samples, due to the bilinear nature of the underlying multi-component FM signal. These cross-terms could be mitigated by designing a low-pass TF kernel in the ambiguity domain that yields maximum output in the direction parallel to the auto-terms and small outputs everywhere else.

Fig. 2(a) shows the real part of the received signal, which contains a total of 96 (i.e., 37.5%) missing samples. These missing samples are clustered into 16 bursts, with each burst having a width of 6 missing samples. Missing data positions are marked with red dots. The corresponding IAF in Fig. 2(b) contains burst missing entries due to burst missing data samples. Figs. 2(c) and 2(d), respectively, show the corresponding AF and WVD, in which aliasing structures, generated due to convolutive sinc-function-like artifact patterns, making spectral estimation and analysis extremely challenging. Unlike the random missing data case, where the artifacts are uniformly distributed in these domains, the artifacts due to burst missing samples exhibit strong patterns and cannot be easily mitigated using adaptive TF kernel alone.

Figs. 3(a)–3(f) provide comparison of the TFRs obtained using different existing approaches, applied to the received signal shown in Fig. 2(a). The TFR in Fig. 3(a), obtained with the MIAA method applied in the IAF domain, shows excessive

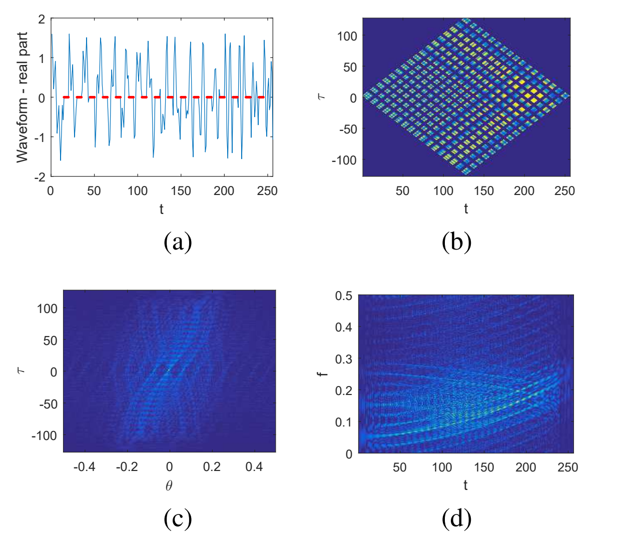

Fig. 2 The received signal with 96 (i.e., 37.5%) missing samples clustered into 16 bursts, each having 6 missing samples: (a) Real part of the signal; (b) IAF; (c) AF; (d) WVD.

cross-terms, similar to the WVD from Fig. 2(d). As observed in Fig. 3(b), the sparse reconstruction based OMP technique, when applied after MIAA, performs poorly when trying recover the true signal components and suppress cross-terms. The AOK in Fig. 3(c) performs relatively well in recovering the strong signal component. However, aliasing at both sides may misguide the identification of the weak signal component. Figs. 3(d) and 3(f) show TFR reconstruction results using

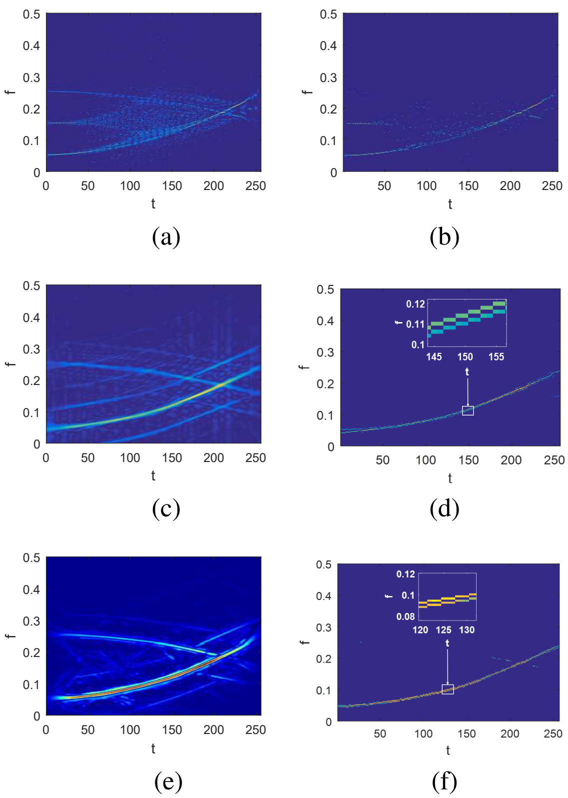

Fig. 3 The TFRs obtained using different existing approaches applied to the received signal of Fig. 2(a): (a) MIAA applied to the IAF; (b) OMP applied after MIAA; (c) AOK; (d) OMP applied to the kerneled IAF obtained from the AOK; (e) ADTFD with WVD as the underlying TFD; (f) OMP applied after the ADTFD.

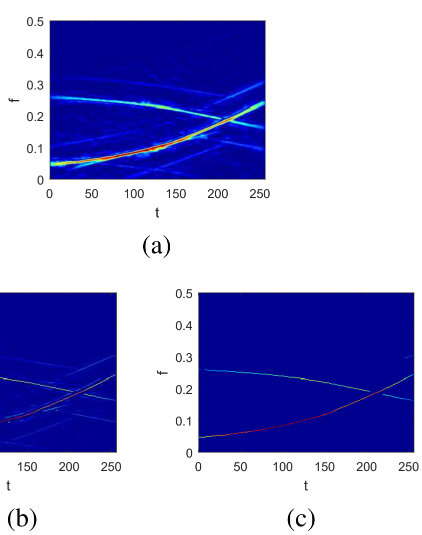

Fig. 4 The TFRs obtained by applying the proposed techniques to the received signal of Fig. 2(a): (a) ADTFD with SPWVD as the underlying TFD; (b) Resulting TFR after smoothing the TFR of Fig. 4(a) using global thresholding; (c) Proposed ALF-DTFD (M=1, Q=256, ξ=0.41).

OMP applied to the IAFs, respectively obtained from the AOK and the ADTFD. In both cases, the OMP fails to recover the weak signal component. The high-energy sinc-like artifact patterns resulted from the burst missing samples, concentrated near the strong signal component in the respective underlying TFRs, are misguided as the second signal component in the OMP, leading to erroneous results. As seen in Fig. 3(e), the ADTFD, using the WVD as the underlying TFD with $p = 2$ and $q = 30$, produces TFR reconstruction results with better artifact suppression compared to all aforementioned approaches. Nevertheless, the artifacts due to burst missing samples and spurious signal signatures near the intersection of the two components remain an issue.

In Fig. 4(a), the SPWVD is used as the underlying TFD instead of WVD while computing ADTFD, where $p = 0.3$, $q = 100$, $h[\tau] = 128$, and $g[u] = 5$ are assumed. As compared to Fig. 3(e), the improvement in terms of the IF resolution and energy concentration of the signal components, particularly for the weak signal component and at the intersection of the components, is clearly observed in Fig. 4(a). Fig. 4(b) shows the resulting TFR after smoothing the TFR of Fig. 4(a) with global thresholding, in which a single threshold is used for the entire TFR. While this approach is successful in removing some of the artifacts, the presence of aliasing signal components makes identification of the true IFs difficult, as one universal threshold does not serve for alias mitigation and auto-term preservation. Fig. 4(c) provides TFR obtained using the proposed ALF-DTFD approach applied to the TFR depicted in Fig. 4(a). The values of M and ξ considered are respectively 1 and 0.41. As evident from Fig. 4(c), the proposed approach not only removes all cross-terms and artifacts due to burst missing data samples, but also preserves high energy and resolution of the auto-terms. This clearly demonstrates the superiority of the proposed technique in pre-processing the TFRs with increased reliability.

V. Conclusions

In this paper, we have developed a novel adaptive local filtering based approach for the TF analysis of multi-component FM signals. The proposed ALF-DTFD is simple, yet effective in removing cross-terms and undesired artifact effects due to burst missing samples, while preserving desired signal auto-terms in the underlying TFR of the multi-component FM signal. When the signal has multiple components that are closely separated or have large variations in their relative amplitudes, the proposed approach is seen to be efficient in resolving weak signal components while preserving a high resolution of the true IFs. The effectiveness of the proposed technique in providing reliable TF signature estimation is successfully demonstrated using a challenging multi-component signal scenario, where the other sparse reconstruction based approaches fail to recover the weak signal component.

References

[1] B. Boashash, "Estimating and interpreting the instantaneous frequency of a signal – part 1: Fundamentals," *Proc. IEEE*, vol. 80, no. 4, pp. 520–538, Apr. 1992.

[2] A. Papandreou-Suppappola (Ed.), *Applications in Time-Frequency Signal Processing*, CRC Press, 2002.

[3] L. Cohen, "Time-frequency distributions – A review," *Proc. IEEE*, vol. 77, no. 7, pp. 941–981, July 1989.

[4] B. Boashash, “Estimating and interpreting the instantaneous frequency of a signal – Part 2: Algorithms and applications,” *Proc. IEEE*, vol. 80, no. 4, pp. 540–568, Apr. 1992.

[5] V. S. Amin, Y. D. Zhang, and B. Himed, “Sparsity-based time-frequency representation of FM signals with burst missing samples,” *Signal Process.*, vol. 155, pp. 25–43, Feb. 2019.

[6] Y. D. Zhang, M. G. Amin, and B. Himed, “Reduced interference time-frequency representations and sparse reconstruction of undersampled data,” in *Proc. European Signal Process. Conf.*, Marrakech, Morocco, Sept. 2013, pp. 1–5.

[7] Q. Wu, Y. D. Zhang, and M. G. Amin, “Continuous structure based Bayesian compressive sensing for sparse reconstruction of time-frequency distributions,” in *Proc. Int. Conf. Digital Signal Process.*, Hong Kong, China, Aug. 2014, pp. 831–836.

[8] L. Stankovic, S. Stankovic, I. Orovic, and Y. D. Zhang, “Time-frequency analysis of micro-Doppler signals based on compressive sensing,” in M. Amin (ed.), *Compressive Sensing for Urban Radars*, CRC Press, 2014.

[9] M. G. Amin, B. Jokanovic, Y. D. Zhang, and F. Ahmad, “A sparsity-perspective to quadratic time-frequency distributions,” *Digital Signal Process.*, vol. 46, pp. 175–190, Nov. 2015.

[10] N. A. Khan and S. Ali, “Sparsity-aware adaptive directional time–frequency distribution for source localization,” *Circuits Syst. Signal Process.*, vol. 37, no. 3, pp. 1223–1242, Mar. 2018.

[11] D. L. Jones and R. G. Baraniuk, “An adaptive optimal-kernel time-frequency representation,” *IEEE Trans. Signal Process.*, vol. 43, no. 10, pp. 2361–2371, Oct. 1995.

[12] J. A. Tropp and A. C. Gilbert, “Signal recovery from random measurements via orthogonal matching pursuit,” *IEEE Trans. Inf. Theory*, vol. 53, no. 12, pp. 4655–4666, Dec. 2007.

[13] Y. D. Zhang, “Resilient quadratic time-frequency distribution for FM signals with gapped missing data,” in *Proc. IEEE Radar Conf.*, Seattle, WA, USA, May 2017, pp. 1765–1769.

[14] P. Stoica, J. Li, and J. Ling, “Missing data recovery via a non-parametric iterative adaptive approach,” *IEEE Signal Process. Lett.*, vol. 16, no. 4, pp. 241–244, Apr. 2009.

[15] N. Khan and B. Boashash, “Multi-component instantaneous frequency estimation using locally adaptive directional time frequency distributions,” *Int. J. Adaptive Control Signal Process.*, vol. 30, pp. 429–442, Mar. 2016.

[16] B. Boashash, N. A. Khan, and T. Ben-Jabeur, “Time-frequency features for pattern recognition using high-resolution TFDs: A tutorial review,” *Digital Signal Process.*, vol. 40, pp. 1–30, May 2015.

[17] B. Boashash (Ed.), *Time-Frequency Signal Analysis and Processing*, 2nd Ed. Academic Press, 2016.

[18] F. Auger and P. Flandrin, “Improving the readability of time-frequency and time-scale representations by the reassignment method,” *IEEE Trans. Signal Process.*, vol. 43, pp. 1068–1089, May 1995.

[19] P. L. Shui, H. Y. Shang, and Y. B. Zhao, “Instantaneous frequency estimation based on directionally smoothed pseudo-Wigner-Ville distribution bank,” *IET Radar Sonar Navig.*, vol. 1, no. 4, pp. 317–325, Aug. 2007.